Evaluation of Controllability of Interaction Between Pedestrian and Autonomous Mobile Robot in Shared Mobility Space

Kentaro Sugiura[a], Mizuho Aoki, Kazuhide Kuroda,
Hiroyuki Okuda[b] and Tatsuya Suzuki[c]
Mechanical Systems Engineering, Nagoya University, Furo-cho, Chikusa, Nagoya, Aichi, Japan

Keywords: Autonomous Mobile Robot (AMR), Pedestrian Behavior, Logistic Regression Model, Controllability.

Abstract: Recently, a growing number of autonomous mobile robots (AMR) coexisting with humans are being introduced in many types of AMR-human shared space. Such AMR often needs to be navigated in narrow spaces while smoothly interacting with pedestrians. In such a situation, AMRs are highly recommended to estimate the pedestrian's intentions and take appropriate action from the viewpoint of social acceptance. First, this paper presents new modeling and understanding of pedestrian behavior, particularly focusing on decision-making when they face an AMR at a close distance. Real-world experiments were conducted using a remote switch to directly record their decisions, and a mathematical decision model is made by using a logistic regression model. In the interaction between AMR and pedestrians, the AMR is expected to 'implicitly control' the interacting pedestrian by changing its own action. From this perspective, the influence of the AMR motion on the pedestrian's decision is formally defined and calculated by using the controllability Gramian of the augmented AMR-pedestrian system model. A deep understanding of the influence of AMR action on pedestrian behavior will be beneficial to develop control policies for smooth AMR-pedestrian interactions.

1 INTRODUCTION

According to the growing demand from decreasing of labor population and advancements in robotic technology, an enormous number of small-scale autonomous mobile robots (AMR) have been implemented in many types of AMR-human shared space. The typical applications are: autonomous electric wheelchairs (Ryu et al., 2022), delivery robots (Boysen et al., 2020), and mobile robots working in factories (Singhal et al., 2017).

A common feature of these AMRs is that they frequently encounter situations where they have to pass by people at close distances, such as narrow space passages. In such a situation, there is a high expectation for the development of AMR that can interact harmoniously with pedestrians without causing any fare nor discomfort.

Numerous studies have been conducted on the passive interactive motion of AMRs that predicts pedestrian movement in advance and avoid interference (Ziebart et al., 2009; Luo et al., 2018; Rudenko et al., 2017; Yang et al., 2018). This approach is effective in terms of enhancing safety and is highly practical for open-space navigations.

On the other hand, the passive policy is not always ideal in the case of a situation where an AMR needs to navigate through a narrow space with interacting oncoming pedestrians. For instance, if an AMR were to stop or shift its direction to avoid obstructing oncoming pedestrians, it could potentially disadvantage those following behind. 'Freezing Robot Problem'(FRP)(Trautman and Krause, 2010), is also getting to be a common problem among robots working near the pedestrian. Robots sometimes can not move since the all candidate paths made by the planner are unsafe in crowded situations with a conventional passive collision avoidance approach. To solve this problem, not only the robot but the closed loop system consisting of the robot and surrounding pedestrian must be considered as the control plant. By considering the closed loop system, the robot can behave to guide the pedestrians in contrast to avoid surrounding pedestrians passively. To realize a mutu-

[a] https://orcid.org/0009-0005-4914-9142
[b] https://orcid.org/0000-0002-2910-4634
[c] https://orcid.org/0000-0002-0182-308X

Sugiura, K., Aoki, M., Kuroda, K., Okuda, H. and Suzuki, T.
Evaluation of Controllability of Interaction Between Pedestrian and Autonomous Mobile Robot in Shared Mobility Space.
DOI: 10.5220/0012177500003543
In *Proceedings of the 20th International Conference on Informatics in Control, Automation and Robotics (ICINCO 2023) - Volume 2*, pages 249-257
ISBN: 978-989-758-670-5; ISSN: 2184-2809

ally beneficial scenario in such cases, AMR should design it in real-time based on surrounding conditions and express its intentions to pedestrians through its movements. In such case, the AMR is desired to take some positive action to induce the pedestrian's behavior to realize smooth interaction. This kind of positive action can be regarded as a part of behavioral negotiation between AMR and pedestrians. In (Eldridge and Maciejewski, 2005), for example, genetic algorithms have been used to design positive action. However, it is unclear if the approach works in environments other than where the strategy was learned. Poor explainability of the policy due to the data-driven approach can also be a problem in actual operations.

To realize behavioral negotiation, this paper develops a model to estimate pedestrian behavior in response to AMR actions. First of all, the experiments on interactive behavior are conducted and data on interactive behavior is obtained from real-world experiments. Since in the interaction, the pedestrian's decision-making plays an important role, the pedestrian's decision such as 'stop' or 'go ahead' is explicitly measured by using the hand-held switch in addition to the position and velocity data. Based on obtained data, a logistic regression model is used to represent the decision-making of the pedestrian mathematically. Moreover, it is crucial for the design of AMR to understand how much is the pedestrian influenced by the AMR's action. The strength of the influence is one of the key elements to deciding whether the AMR takes passive or active action.

In this paper, the quantitative index which represents the degree of influence in the interaction, i.e., how much the AMR's action affects on the pedestrian's behavior is proposed by using the controllability Gramian (Imran and Ghafoor, 2015; Zhao and Pasqualetti, 2017; Nozari, 2020; Roy and Xue, 2019) of the augmented AMR-pedestrian system model. It is known that the magnitude of the eigenvalues of the controllability Gramian W_c corresponds to the size of the reachable set, and from this, $tr(W_c)$, which is the sum of the eigenvalues of W_c, can be used as an index to measure the controllability of the system. Although the original augmented AMR-pedestrian model has nonlinearity, the controllability Gramian was calculated by linearizing the original system model.

In summary, the two main contributions of this study are listed as follows,

- To quantify the influence of AMR motion on pedestrians, an analysis based on a controllability Gramian is proposed.

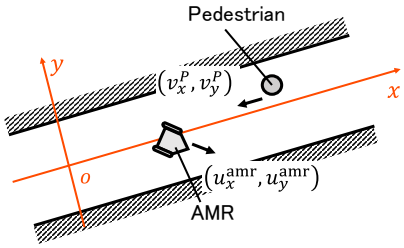

(a) Definition of the coordinate system for explanatory variables input to the model

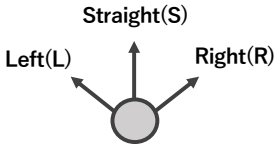

(b) Three hypothetical decisions

Figure 1: Target task and definition of intention.

- The experiment was conducted on a real-world narrow path with both AMR and pedestrian traffic. The pedestrian intention was directly acquired via a hand-held device to achieve both simplicity and accuracy of the prediction model.

2 QUANTIFICATION OF CONTROLLABILITY OF PEDESTRIAN MOTION

This study proposes an evaluation index that quantifies by how much the pedestrian's motion is affected by the action of minimal mobility. In this section, the target task and the definition of the variables are explained first, then the decision model of the pedestrian is introduced, and the controllability Gramian is utilized as the evaluation index of the controllability of human motion, which is an input to the AMR. Finally, the setup of an experiment for directly recording human decisions is explained.

2.1 Target Task and Variable Definition

Figure 1 shows the target task assumed in this study. In Fig. 1, the target AMR is moving down the corridor and one pedestrian is moving up towards the AMR. Although multiple pedestrians must be considered for real-world applications, this study adopts a situation in which only one strain exists to simplify the problem and examine the proposed concept. The definition of the measured variables in Fig. 1 are listed in Table 1.

Table 1: Definition of variables for the pedestrian model.

Absolute velocity of AMR	$u_x^{\mathrm{amr}}, u_y^{\mathrm{amr}}$	[m/s]
Absolute velocity of pedestrian	v_x^P, v_y^P	[m/s]
Relative position of AMR	$x^{\mathrm{amr,rel}}, y^{\mathrm{amr,rel}}$	[m]
Relative velocity of AMR	$v_x^{\mathrm{amr,rel}}, v_y^{\mathrm{amr,rel}}$	[m/s]
Distance between pedestrian and wall	d	[m]

Here, it is assumed that the approaching pedestrian has a descritized intention in the following three states (see Fig. 2. Each broken line represents the output probability at that step, and the most probable intention is defined as the intention at that step:)

- Going right from current position $(D(t) = \boldsymbol{R})$,
- Going left from current position $(D(t) = \boldsymbol{L})$,
- Going straight $(D(t) = \boldsymbol{S})$,

where $D(t) \in \{\boldsymbol{R}, \boldsymbol{L}, \boldsymbol{S}\}$ is the intention of the approaching pedestrian at the time.

2.2 Decision Making and Motion Model for Pedestrian

Next, a decision model of the pedestrian is used to mathematically represent the pedestrian's intention selection. A wide variety of human decision models have been proposed in conventional studies; however, in this study, a logistic regression model is used for ease of mathematical derivation explained later. First, the objective variable of the model y with five explanatory variables and three events $G_i (i = R, L, S)$ is defined as follows;

$$\boldsymbol{x} = [x^{\mathrm{amr,rel}}, y^{\mathrm{amr,rel}}, v_x^{\mathrm{amr,rel}}, v_y^{\mathrm{amr,rel}}, d]^\top, \quad (1)$$

$$y \in \{R, L, S\}, \quad (2)$$

where $x^{amr,rel}, y^{amr,rel}, v_x^{amr,rel}$, and $v_y^{amr,rel}$ are the relative positions and velocities of AMR from the pedestrian in the x and y directions, respectively.

When the measured data $\boldsymbol{x}$ is obtained, the probability $P(G_k)$ that this data belongs to event $G_k (k = R, L)$ and the probability G_S can be expressed as follows;

$$P(G_k) = \frac{\exp(\boldsymbol{\eta}_k \boldsymbol{x})}{1 + \sum_{r \in \{R,L\}} \exp(\boldsymbol{\eta}_r \boldsymbol{x})} (^\forall k \in \{R, L\}), \quad (3)$$

$$P(G_S) = \frac{1}{1 + \sum_{r \in \{R,L\}} \exp(\boldsymbol{\eta}_r \boldsymbol{x})}. \quad (4)$$

Where $\boldsymbol{\eta_k}$ is the coefficient vector estimated from learning data using the maximum likelihood estimation method (Peng et al., 2002).

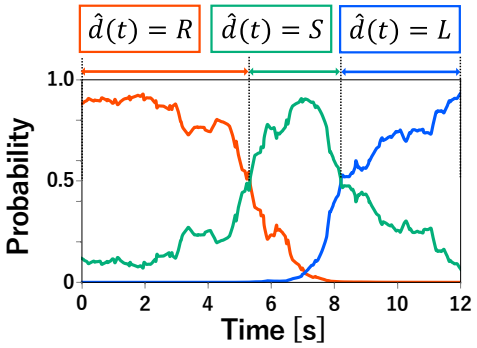

Figure 2: Definition of intention and example of the intention estimation using the obtained Model.

The logistic regression model considers the explanatory variables as inputs, whereas the classification probabilities of the objective variables are considered as the outputs. Thus, the logistic regression model can express the ambiguity of human decisions owing to its ability to use the classification probability of the objective variable as its output. In addition, since the logistic regression model cannot represent complex structures compared to neural networks (de Brito et al., 2021; Hasan et al., 2018; Eiffert et al., 2020), the explainability of the input-output relationship increases the explainability of the model. This can be a significant advantage for prospects in path planning. Furthermore, since this study primarily focuses on analysis, the high explainability of the model has significant implications. Therefore, this study employed logistic regression to construct a model that can estimate the pedestrian's decision(Watanabe et al., 2023; Zhao et al., 2019; Nor et al., 2017).

The estimated intention $\hat{D}(t)$(see Fig. 1b) at t can be computed as the intention with the highest probability by the following equation:

$$\hat{D}(t) = \arg\max_{r \in \{R,L,S\}} P(D(t) = r | \boldsymbol{\phi}(t).\boldsymbol{\eta}_r). \quad (5)$$

where $\boldsymbol{\phi}(t)$ is the extended regressor vector consisting of explanatory variables. Pedestrian motion is also defined here based on the estimated intention. The velocity of the pedestrian is computed as the weighted sum of the reference speed for each intention as fol-

lows;

$$\begin{bmatrix} v_x^P \\ v_y^P \end{bmatrix}_k = \begin{bmatrix} V_{xR}^{\mathrm{ref}} & V_{xL}^{\mathrm{ref}} & V_{xS}^{\mathrm{ref}} \\ V_{yR}^{\mathrm{ref}} & V_{yL}^{\mathrm{ref}} & V_{yS}^{\mathrm{ref}} \end{bmatrix} \begin{bmatrix} P(G_R) \\ P(G_L) \\ P(G_S) \end{bmatrix}_k, \quad (6)$$

where V_{iJ}^{ref} is the reference speed in direction i in the intention $D(t) = J$. The magnitude of the speed $\|V^{ref}\|$ was set to 1.0 m/s, whereas the angle between the horizontal axis x and direction of the speed was set to $\pi/4$, $-\pi/4$, and 0, for each intention.

2.3 Pedestrian Controllability Index Based on Controllability Gramian

The interaction between the human pedestrian and AMR must be considered when designing the motion plan of an AMR. However, the quantitative index of the intensity of the interaction, i.e. by how much the pedestrian is affected by the motion of the AMR, is not discussed in conventional studies, whereas a simple physical measure, such as distance and/or direction, is used. In this study, the quantitative evaluation index of the controllability of the pedestrian's behavior is proposed to investigate the intensity of the interaction and how the pedestrian is affected by the AMR's behavior. The relationship between them is represented as a local linear system based on a mathematical model, and the controllability is discussed when the AMR's velocity is considered as the input and the pedestrian's velocity is the state. To analyze the relationship between AMR and pedestrian velocity change, a bivariate Taylor expansion is performed on the AMR velocity vectors $v_x^{\mathrm{amr,rel}}, v_y^{\mathrm{amr,rel}}$ for the pedestrian among the explanatory variables of the model. Since the respective classification probabilities are expressed in (3) and (4), a bivariate Taylor expansion of the logistic regression model can be written as follows:

$$P(G_R) = w_{R,v_x} v_x^{amr,rel} + w_{R,v_y} v_y^{amr,rel} + w_{R,C}, \quad (7)$$

$$P(G_L) = w_{L,v_x} v_x^{amr,rel} + w_{L,v_y} v_y^{amr,rel} + w_{L,C}, \quad (8)$$

$$P(G_S) = w_{S,v_x} v_x^{amr,rel} + w_{S,v_y} v_y^{amr,rel} + w_{S,C}, \quad (9)$$

where $w_{D,*}$ is the constant weight parameters.

Considering of pedestrian behavior model (6) with a first-order delay for the behavior, a local behavior is approximately linearized as follows:

$$\begin{aligned} \begin{bmatrix} x^P \\ y^P \\ v_x^P \\ v_y^P \end{bmatrix}_{k+1} &= \begin{bmatrix} 1 & 0 & \Delta t & 0 \\ 0 & 1 & 0 & \Delta t \\ 0 & 0 & 0 & 0 \\ 0 & 0 & 0 & 0 \end{bmatrix} \begin{bmatrix} x^P \\ y^P \\ v_x^P \\ v_y^P \end{bmatrix}_k \\ &+ \begin{bmatrix} 0 & 0 & 0 \\ 0 & 0 & 0 \\ V_{xR}^{ref} & V_{xL}^{ref} & V_{xS}^{ref} \\ V_{yR}^{ref} & V_{yL}^{ref} & V_{yS}^{ref} \end{bmatrix} \begin{bmatrix} P(G_R) \\ P(G_L) \\ P(G_S) \end{bmatrix}_k, \end{aligned} \quad (10)$$

Substituting (7), (8), and (9),

$$\begin{aligned} \begin{bmatrix} x^P \\ y^P \\ v_x^P \\ v_y^P \end{bmatrix}_{k+1} &= A'_k \boldsymbol{x_k} + \begin{bmatrix} 0 & 0 & 0 \\ 0 & 0 & 0 \\ \xi_{x0} & \xi_{x1} & \xi_{x2} \\ \xi_{y0} & \xi_{y1} & \xi_{y2} \end{bmatrix}_k \begin{bmatrix} v_x^{amr,rel} \\ v_y^{amr,rel} \\ 1 \end{bmatrix}_k, \\ &= A'_k \boldsymbol{x_k} + \begin{bmatrix} 0 & 0 & 0 \\ 0 & 0 & 0 \\ \xi_{x0} & \xi_{x1} & \xi_{x2} \\ \xi_{y0} & \xi_{y1} & \xi_{y2} \end{bmatrix}_k \begin{bmatrix} u_x^{amr} - v_x^P \\ u_y^{amr} - v_y^P \\ 1 \end{bmatrix}_k, \\ &= \begin{bmatrix} 1 & 0 & \Delta t & 0 \\ 0 & 1 & 0 & \Delta t \\ 0 & 0 & -\xi_{x0} & -\xi_{x1} \\ 0 & 0 & -\xi_{y0} & -\xi_{y1} \end{bmatrix}_k \begin{bmatrix} x^P \\ y^P \\ v_x^P \\ v_y^P \end{bmatrix}_k + B_k \boldsymbol{u}_k, \\ &= A_k \boldsymbol{x}_k + B_k \boldsymbol{u}_k, \end{aligned} \quad (11)$$

where $v^{\mathrm{amr,rel}}$ is the relative velocity of the AMR to the pedestrian, v^P is the velocity of the pedestrian in global coodinate, and u is the input velocity of the AMR in the global coodinate.

The controllability Gramian $W_c(t)$ can be defined by the state transition matrix A_k and the input matrix B_k in the linear approximation system. The magnitude of the eigenvalues of the controllability Gramian $W_c(t)$ corresponds to the size of the reachable set, and thus $tr(W_c(t))$ (the sum of eigenvalues of the controllability Gramian) is used as an indicator of the controllability in a system (Imran and Ghafoor, 2015). The general formula of the controllability Gramian for a given discrete-time linear state space system can be expressed as follows (Zhao and Pasqualetti, 2017):

$$W_c^{\infty}(t) = \sum_{i=0}^{\infty} A_k^i B_k B_k^{\top} (A_k^{\top})^i. \quad (12)$$

However, the linear system in this study uses a local approximation at a time t, and it is difficult to account for controllability over an infinite number of steps. Therefore, the controllability Gramian for a finite number of steps, $W_c^L(t)$, defined by the following equation is used instead (Roy and Xue, 2019;

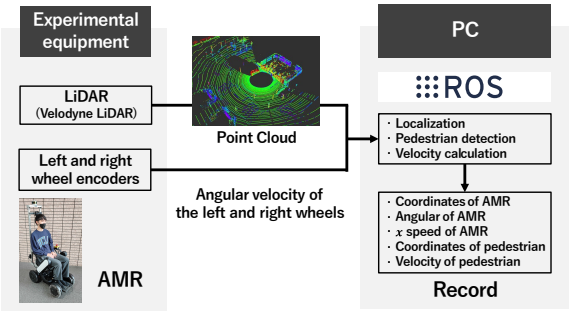

Figure 3: Experiment machine configuration.

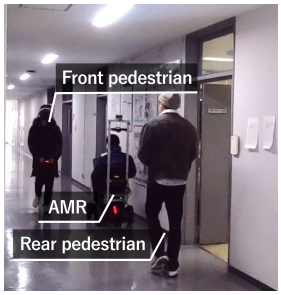

(a) Actual image of experiment

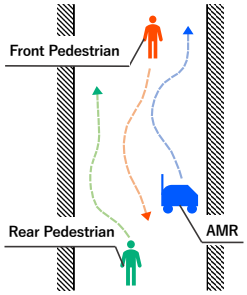

(b) Top view illustration

Figure 4: Observation experiment of pedestrian behavior.

Nozari, 2020):

$$W_c^L(t) = \sum_{i=0}^{L-1} A_k^i B_k B_k^\top (A_k^\top)^i \tag{13}$$

where the L is the number of steps that the controllability is evaluated.

The linear system in this study includes non-quadratic terms in the input. Since controllability is an indicator of the impact of input changes on the state, the controllability of the pedestrian's velocity on the AMR velocity is considered without a constant term. Since the time interval between each steps, Δt, is set to 80 ms and $L = 13$ is applied, the evaluation duration $L\Delta t \approx 1s$.

Hence, the index required to evaluate the intensity of the interaction between the AMR and the pedestrian P is defined by the trace of the computed controllability Gramian $W_c^L(t)$ as follows:

$$J_{cg}^{P,AMR}(t) = \mathrm{tr}\left(W_c^L(t)\right). \tag{14}$$

$J_{cg}^{P,AMR}(t)$ is the scalar value and quantifies by how much the AMR's movement affects the pedestrian's motion.

3 EXPERIMENT FOR MODELING PEDESTRIAN BEHAVIOR

3.1 Experimental Setup

Figure.3 shows a schematic diagram of the experimental system in the human behavior observation. This experiment aims to obtain the learning data required to construct a decision model (5) for an oncoming pedestrian. The pedestrian's decisions at each step in response to the AMR's behavior are required when pedestrians and the AMR face each other. Data acquisition experiments are conducted in typical narrow passages that exist indoors as shown in Fig. 4a.

Table 2: Instructions for the AMR operator.

1	Walking on the left side of the path
2	Walking on the center of the path
3	Walking on the right side of the path

The experiment consists of three participants: an electric wheelchair with a human operator (hereinafter referred to as 'AMR'), a pedestrian facing the AMR, and a pedestrian walking along the path of the AMR from behind (see Fig. 4b). The two pedestrians start walking according to the cue, pass each other, and finish walking, each of which is considered as one trial. Four pair of the front and rear pedestrian performed 81 trials for each, then 324 trials are measured in total. The starting positions of the three participants were specified randomly for each trial. The AMR operator was given additional instructions regarding their actions as the operator of the experiment (Table 2) to vary the situations. The other subjects were not given instructions, and directed to act as usual.

3.2 Pedestrian's Behavior Observation

A 3D-LiDAR sensor was used to record the position and speed information, which is derived by differentiating the pedestrian's position, of the pedestrians. The point cloud data were clustered to identify and record the pedestrians. For recording the dependent variable, which is the intention of the pedestrian facing the AMR, the buttons on the pedestrian's controller were used to directly record their inputs. Table 3 lists the recorded data.

The observed data are transformed into explanatory variables used for model training. The transformed coordinates are the horizontal and vertical axes of the passage shown in Fig. 5. Furthermore, an example of the trajectories of the three participants is shown in Fig. 6.

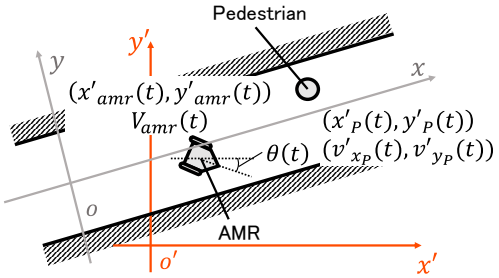

Figure 5: Definition of coordinates and measured variables.

Table 3: Definition of observed variables.

AMR's position	x'_{amr}, y'_{amr}	[m]
AMR's speed	V_{amr}	[m/s]
AMR's rotation angle	θ	[rad]
Pedestrian's position	x'_p, y'_p	[m]
Pedestrian's velocity	v'_{x_p}, v'_{y_p}	[m/s]
Distance between AMR and wall	d	[m]
Pedestrian's intention	$D(t)$	

4 RESULTS OF EVALUATION

4.1 Evaluation of Decision Model of Oncoming Pedestrian

Because the evaluation index of the controllability proposed in this study utilizes the behavior model of the pedestrian interacting with AMR, the accuracy of the model must be realistic. The accuracy of the model was evaluated based on the matching rate between the recorded intention and that estimated by the model. The obtained model exhibited a matching rate of 88.8%. This value is not perfect; however, it can be regarded as sufficiently high to investigate the characteristics of the obtained behavior model. Note that the proposed index described in the section 2.3 can also be applied for different types of behavior models provided the model can be derived. Simple neural network models can be used if the modeling accuracy is a priority, whereas this study applied the logistic regression model for simplicity. Figure 7 shows a comparison of the recorded and the estimated intentions using the model under the same trial. Although the estimation around the decision timing (switching point) is not accurate, it was confirmed that the trend is nearly similar to the recorded one.

4.2 Evaluation of Controllability of Pedestrian's Motion

The controllability index $J_{cg}^{P,AMR}(t)$ is the scalar value since it is computed from the trace of the controllability Gramians of the linearized human behavior model (section 2.3.) Here we call the trace value of the controllability Gramian 'controllability index' as the proposed index to evaluate the controllability of the pedestrian's motion on the AMR's behavior. The larger the $J_{cg}^{P,AMR}(t)$, the higher the controllability, and the smaller the $J_{cg}^{P,AMR}(t)$, the lower the controllability. Figures 8 to 9 show the results of computing the controllability index at each pedestrian position when the AMR is located at the depicted position. The values shown in those figures are normalized among all situations.

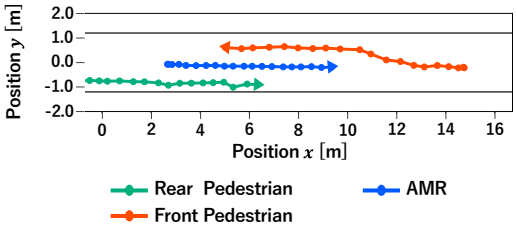

The AMR operator drives straight to right, and the front pedestrian avoids the collision by changing its walking path.

Figure 6: Example of the observed trajectory of three participants.

(a) Observed intention

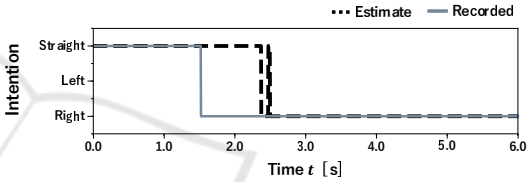

(b) Comparison between time profiles of observed intention and estimated intention

Figure 7: Comparison of recorded intentions and model estimation.

4.3 Relationship Between Decisions and Controllability

Figure 8(a) shows the estimated intention of the pedestrian by the model constructed in the previous section. Red, blue, and green colors indicate the estimated pedestrian's intention to turn right, turn left, and keep going straight, respectively. Figure 8(b) shows the result of computing the controllability index when the AMR traveled straight toward the $x+$ direction with 1.0m/s from the center of the path.

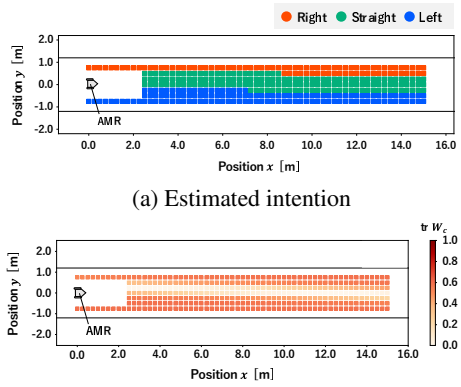

(a) Estimated intention

(b) Controllability

Figure 8: Relationship between decision making and controllability.

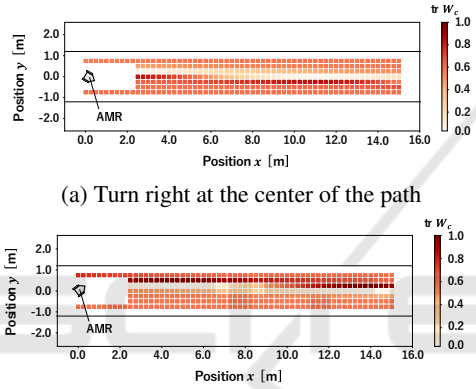

(a) Turn right at the center of the path

(b) Turn left at the center of the path

Figure 9: Controllability of pedestrians when AMR changes its driving path.

Generally, the controllability index shows a higher value when pedestrians are located on both sides of the path. This is because the collision risk is higher at both ends of the aisle compared to the center part, and the pedestrian is sensitive to AMR's actions. When a pedestrian is positioned on either side of the path, there is only one direction to escape. This means that the pedestrian can make a clear decision in this case, and the relationship between the AMR and the pedestrian's motion becomes clear too.

In contrast, from Fig. 8, the result shows less controllability in the area where the pedestrian is located at the center of the path. In this area, although the decision model shows the pedestrian is going straight, this includes two cases; the pedestrian is going straight, or, is unsure of his/her decision. This means that the pedestrian is free to select the route to avoid the AMR at the center of the path. At first glance, this freedom for decision-making seems to lead to more controllability because it may result in more variety in future situations. However, the decision strongly depends on the stochasticity of the pedestrian's random decision and is not controllable by the AMR. Therefore, the pedestrian is not affected so much by the AMR when the pedestrian is located at the center of the path. Note that this result does not imply that the controllability index could be decreased even in a situation with strong interaction if the AMR's motion and the pedestrian's motion are independent of each other.

4.4 Discussion on Effect of Changing AMR's Behavior

Figure 9 show the cases when the AMR is turning right and left from the center of the pass, respectively.

Figure 9 shows that the controllability is large when the AMR changed its course and the pedestrian is positioned ahead of the AMR's direction. On the left-hand side of the AMR in Figure 9(a), it can be seen that the controllability index on the right-hand side of the AMR in the path (bottom in the figure) is relatively larger than those on the left-hand side (top in the figure). In contrast, in Figure 9(b), the result shows that the controllability index on the left-hand side of the AMR is higher than the opposite side. This is because the pedestrian senses the collision risk and avoids the collision with AMR. From the pedestrian's viewpoint, the AMR's intention becomes clear when the AMR changes its course toward the pedestrian. As a result, the pedestrian changes their destination to avoid collision with the AMR. In contrast, when the pedestrian is not positioned ahead of the AMR, the pedestrian will not change their intention depending on the AMR's motion, but follow his/her intention. This reduces the intensity of the interaction, that is, controllability.

5 APPLICATION OF CONTROLLABILITY INDEX

This section introduces an application of the proposed index for planning the actions of AMR. An example of action planning based on this concept is discussed to demonstrate the potential of the controllability index. The example takes controllability into account in the social force model (SFM) (Helbing and Molnar, 1995; Iwamura et al., 2016; Helbing and Molnár, 1995; Wu et al., 2022). Two contrasting hypotheses on positive actions with controllability were examined only with limited demonstrations. The appropriateness of the two hypotheses was not considered

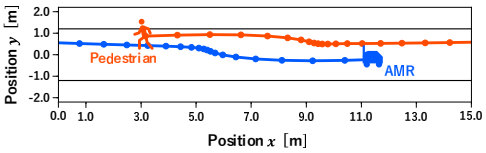

Figure 10: Standard SFM without considering the controllability index.

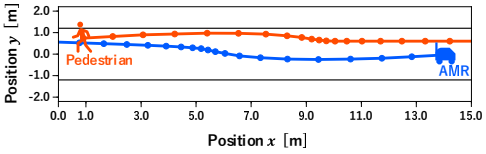

Figure 11: AMR's model for proactive action (Model A).

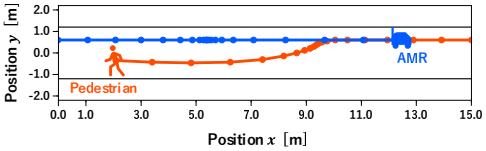

Figure 12: AMR's model for conservative action (Model B) (See also the video at https://youtu.be/pAdprVS3i14).

in this study; however, it will be covered in future investigations. Here the action planning consistent with the following two hypotheses was tested;

- When the controllability is high, the AMR's active behavior is considered to indicate its intention to act and guide the pedestrian. Therefore, the action planning should facilitate the active movement of the AMR when the controllability is high.
- When controllability is high, the AMR's behavior may destabilize the pedestrian's judgment. Therefore, the action planning should RESTRICT active AMR movement when the controllability is high.

The SFM that considers the two hypotheses above (Models A and B refer to the controller model based on hypotheses 1 and 2, respectively.) and the standard SFM that does not consider the controllability index are compared in the numerical simulation. Along with the standard SFM, a pedestrian model that includes the intention as a reference velocity is used. The simulation increased the lateral sensitivity to the lateral force of the AMR by 1.3 times for Model A and decreased it by 1/10 for Model B when the controllability index exceeded a certain threshold value. Figures 10, 11 and 12 show the simulation results. The points depict the time evolution of the simulation and the time between each position was 0.5 seconds.

First, a comparative analysis was conducted between the standard SFM and Model A. The AMR moved actively, which indicates its intention to the pedestrian via its action and simplifies the pedestrian's decision on the avoidance direction. The point density on the steps before and after the pedestrian initiates avoidance of Model A and the standard SFM were compared. The result showed that Model A exhibits a lower point density, i.e. a higher passing speed. Second, a comparison was conducted between Model A and Model B. The two models exhibited a significant difference in their paths. While AMR with Model A changed direction rapidly, the other model did not change direction. The pedestrian's direction of avoidance also showed the difference between Models A and B. In the case of Model A, the AMR changed its direction and the pedestrian could easily decide since the AMR's intention was clear. In contrast, the pedestrian in Model B changed direction because the pedestrian observed that the AMR did not change its direction. Under hypothesis 2, high controllability index might indicate that the pedestrian's decision was sensitive and unstable. For Model B, the AMR did not change direction to avoid disturbing the decision of the pedestrian.

The controllability index, proposed in this study, is important in constructing a motion planner that is more efficient, safer, and human-friendly. Our goal in the future is to compare the effectiveness of different hypotheses using the controllability index as a factor in an optimization problem for action planning, and ensuring a friendly AMR that considers surrounding pedestrians.

6 CONCLUSION

In this paper, the AMR-pedestrian interaction was analyzed based on real-world experiments. In the experiments, pedestrians and AMR passed by in a narrow space. The pedestrian decision-making model was developed using logistic regression. The accuracy of the model was 88.8 %. In addition, the influence of the AMR action on the pedestrian's behavior has been analyzed quantitatively by using the controllability Gramian of the augmented AMR-pedestrian system model. As a result, it was found that the controllability was high when pedestrians were on both sides of the path, and low when pedestrians were in the center of the path. Furthermore, it was found that the controllability was high when the AMR changed its course and the pedestrian was positioned ahead of the AMR's direction. This study explored the potential implications of using a simple model of the controllability of the interaction. This analysis is expected to design smooth interactions between AMRs and pedestrians by understanding how AMRs' actions affect on pedestrians' behavior.

There are numerous challenges to be addressed in the future for the work. Especially, following three points can be mentioned. The first is to clarify the relationship between controllability and the characteristics of pedestrian's decision making to verify the hypothesis proposed in this paper. The second is a improvement of the model accuracy by reconsideration of the model structure and its explanatory variables. The third is to explore an application of the proposed evaluation index. How to make a decision and/or motion of the robots can be developed in the future by utilizing the motion planning and the control method based on the controllability of the human behavior.

ACKNOWLEDGEMENTS

This work is supported by Toyota Motor Corporation, 1 Toyota-Cho, Toyota City, Aichi Prefecture 471-8571, Japan

REFERENCES

Boysen, N., Fedtke, S., and Schwerdfeger, S. (2020). Last-mile delivery concepts: a survey from an operational research perspective. *in OR Spectrum*, 43:1–58.

de Brito, B. F., Zhu, H., Pan, W., and Alonso-Mora, J. (2021). Social-vrnn: One-shot multi-modal trajectory prediction for interacting pedestrians. *Conf. on Robot Learning*, pages 862–872.

Eiffert, S., Li, K., Shan, M., Worrall, S., Sukkarieh, S., and Nebot, E. M. (2020). Probabilistic crowd gan: Multimodal pedestrian trajectory prediction using a graph vehicle-pedestrian attention network. *IEEE Robotics and Automation Letters*, 5:5026–5033.

Eldridge, B. and Maciejewski, A. (2005). Using genetic algorithms to optimize social robot behavior for improved pedestrian flow. *2005 IEEE Int'l Conf. on Sys., Man and Cybernetics*, 1:524–529.

Hasan, I., Setti, F., Tsesmelis, T., Del Bue, A., Galasso, F., and Cristani, M. (2018). Mx-lstm: mixing tracklets and vislets to jointly forecast trajectories and head poses. *Proc. of the IEEE Conf. on Computer Vision and Pattern Recognition*, pages 6067–6076.

Helbing and Molnár (1995). Social force model for pedestrian dynamics. *Physical review. E, Statistical physics, plasmas, fluids, and related interdisciplinary topics*, 51 5:4282–4286.

Helbing, D. and Molnar, P. (1995). Social force model for pedestrian dynamics. *Physical review E*, 51(5):4282.

Imran, M. and Ghafoor, A. (2015). Model reduction of descriptor systems using frequency limited gramians. *J. of the Franklin Institute*, 352(1):33–51.

Iwamura, K., Chen, J., Tanimizu, Y., and Sugimura, N. (2016). A study on transportation processes of autonomous distributed agv based on social force model. *2016 Int'l Symposium on Flexible Automation (ISFA)*, pages 206–209.

Luo, Y., Cai, P., Bera, A., Hsu, D., Lee, W. S., and Manocha, D. (2018). Porca: Modeling and planning for autonomous driving among many pedestrians. *IEEE Robotics and Automation Letters*, 3(4):3418–3425.

Nor, S. N. M., Daniel, B. D., Hamidun, R., Al Bargi, W. A., Rohani, M. M., Prasetijo, J., Aman, M. Y., and Ambak, K. (2017). Analysis of pedestrian gap acceptance and crossing decision in kuala lumpur. *MATEC Web of Conf.*, 103:08014.

Nozari, E. (2020). Lecture 3: Stability, controllability & observability.

Peng, J., Lee, K., and Ingersoll, G. (2002). An introduction to logistic regression analysis and reporting. *J. of Educational Research - J EDUC RES*, 96:3–14.

Roy, S. and Xue, M. (2019). Controllability-gramian submatrices for a network consensus model. *2019 IEEE 58th Conf. on Decision and Control (CDC)*, pages 6080–6085.

Rudenko, A., Palmieri, L., and Arras, K. O. (2017). Predictive planning for a mobile robot in human environments. *Proc. of the Workshop on AI Planning and Robotics: Challenges and Methods (at ICRA 2017), Singapore*.

Ryu, H. Y., Kwon, J. S., Lim, J. H., Kim, A. H., Baek, S. J., and Kim, J. W. (2022). Development of an autonomous driving smart wheelchair for the physically weak. *in Applied Sciences*, 12(1).

Singhal, A., Pallav, P., Kejriwal, N., Choudhury, S., Kumar, S., and Sinha, R. (2017). Managing a fleet of autonomous mobile robots (amr) using cloud robotics platform. *2017 European Conf. on Mobile Robots (ECMR)*, pages 1–6.

Trautman, P. and Krause, A. (2010). Unfreezing the robot: Navigation in dense, interacting crowds. pages 797–803.

Watanabe, T., Yamaguchi, T., Okuda, H., Suzuki, T., Wakisaka, R., and Ban, K. (2023). Analysis and modeling of traffic participants considering interactions at intersections without traffic signals. *2023 IEEE/SICE Int'l Symposium on Sys. Integration (SII)*, pages 1–8.

Wu, W., Chen, M., Li, J., Liu, B., and Zheng, X. (2022). An extended social force model via pedestrian heterogeneity affecting the self-driven force. *IEEE T. on Intelligent Transportation Sys.*, 23:7974–7986.

Yang, C., Tang, Y., Zhou, L., and Ma, X. (2018). Complete coverage path planning based on bioinspired neural network and pedestrian location prediction. pages 528–533.

Zhao, J., Malenje, J. O., Tang, Y., and Han, Y. (2019). Gap acceptance probability model for pedestrians at unsignalized mid-block crosswalks based on logistic regression. *Accident Analysis & Prevention*, 129:76–83.

Zhao, S. and Pasqualetti, F. (2017). Discrete-time dynamical networks with diagonal controllability gramian. *IFAC-PapersOnLine*, 50(1):8297–8302.

Ziebart, B. D., Ratliff, N., Gallagher, G., Mertz, C., Peterson, K., Bagnell, J. A., Hebert, M., Dey, A. K., and Srinivasa, S. (2009). Planning-based prediction for pedestrians. *2009 IEEE/RSJ Int'l Conf. on Intelligent Robots and Sys.*, pages 3931–3936.